Research Article | Vol. 31, No. 17 / 14 Aug 2023 / Optics Express 27296
Optics EXPRESS

Rapidly tunable femtosecond near-UV pulses from a non-collinear optical parametric oscillator

FRIDOLIN JAKOB GEESMANN,[1,2,*] ROBIN MEVERT,[1,2] DAVID ZUBER,[1,2] AND UWE MORGNER[1,2,3]

[1]Institute of Quantum Optics, Leibniz University Hannover, Welfengarten 1, 30167 Hannover, Germany
[2]Cluster of Excellence PhoenixD (Photonics, Optics, and Engineering-Innovation Across Disciplines), 30167 Hannover, Germany
[3]Laser Zentrum Hannover e.V., Hollerithallee 8, 30419 Hannover, Germany
[*]geesmann@iqo.uni-hannover.de

Abstract: Broadband tunable femtosecond laser pulses are of great interest in numerous fields, such as spectroscopy or imaging. Here, we report on the generation of rapidly tunable radiation in the near UV by using intracavity non-collinear sum-frequency mixing between the visible pulses of a non-collinear optical parametric oscillator (NOPO) and a near-infrared beam. The NOPO is pumped by the third harmonic of an Yb-based master oscillator fiber amplifier (MOFA). For sum-frequency mixing, remaining fundamental pulses at 1030 nm are used. With this approach, near-UV pulses in a range of 333-413 nm with average output powers up to 90 mW and pulse durations from 158-240 fs are achieved. Fast tunability is demonstrated over the whole tuning range by varying just the cavity length. The system also allows for the generation of two simultaneous synchronized output pulse trains in the visible and the near-UV spectral range.

Published by Optica Publishing Group under the terms of the Creative Commons Attribution 4.0 License. Further distribution of this work must maintain attribution to the author(s) and the published article's title, journal citation, and DOI.

1. Introduction

Optical parametric oscillators (OPOs) [1,2] enable the generation of laser pulses tunable in wavelength over wide spectral ranges. This has already been demonstrated from the ultraviolet to the mid-infrared [3–7]. However, OPOs have the disadvantage that phase matching is only possible for a small spectral range. It must therefore be adjusted separately for each wavelength in order to tune the OPO. Typical methods to accomplish this are angle [5] or temperature [8] tuning. The achievable tuning speed of such techniques is rather low, as even in fully automated systems typically several seconds are needed for tuning over the entire wavelength range of a few hundred nanometers. An approach for reaching higher tuning speeds is to use a non-collinear geometry, where phase matching is realized over a broad spectral range. In this case, angles and temperature can be kept constant during the tuning process. Hence, changing the wavelength is possible by varying the cavity length only, as it allows to change the temporal overlap between the short pump pulses and the parametric fluorescence broadened by sufficient dispersion inside the resonator. As a result, high tuning speeds can be obtained by mechanically changing the cavity length. Such a system is referred to as a non-collinear optical parametric oscillator. Several publications have already successfully demonstrated NOPOs in the near-infrared [9] or visible [10–12] spectral range with possible tuning velocities for continuous wavelength changes in the order of 100 nm/ms [13]. Even faster wavelength variations in the order of 1000 nm/ms were achieved for ultrafast switching between two wavelengths [14]. In both cases, the process is limited by mechanical constraints only. These properties make NOPOs perfect tools for numerous

#498170 https://doi.org/10.1364/OE.498170
Journal © 2023 Received 15 Jun 2023; revised 15 Jul 2023; accepted 18 Jul 2023; published 31 Jul 2023

Optics EXPRESS

applications, such as real-time stimulated Raman spectroscopy [15] or fast functional imaging [12].

The goal of this work is to extend the spectral range covered by NOPOs towards ultraviolet wavelengths, as this enables the application of various techniques such as resonance Raman spectroscopy [16]. For this purpose, intracavity non-collinear sum-frequency up-conversion with the visible pulses of a NOPO and a near-infrared beam is used to generate quickly tunable femtosecond laser pulses.

2. Experimental setup

An overview of the setup used in this work is shown in Fig. 1. Fundamental pulses with a wavelength of 1030 nm, pulse duration of 250 fs and average output power of up to 15.3 W with a repetition rate of 50.2 MHz are generated by an Yb-based MOFA system. The third harmonic of the near-infrared light is created by the cascaded use of two type-I phase matching processes. For this, the fundamental pulses are first split between two arms using a half-wave plate in combination with a thin-film polarizer. Next, a BBO crystal ($\theta = 23.2°$, $L = 1.5$ mm) is placed in one of the arms to generate the second harmonic at 515 nm, which is subsequently mixed with fundamental pulses from the other arm to produce the third harmonic in a second BBO crystal ($\theta = 32.5°$, $L = 1$ mm). With this approach, output powers of approximately 3.2 W are achieved at a wavelength of 343 nm, corresponding to an optical-to-optical conversion efficiency of 20.9 %. The generated ultraviolet light is then used as a pump for the NOPO, which is designed as a ring resonator. Such a setup is advantageous in our case compared to a standing-wave cavity since the amplification in parametric processes only takes place along one propagation direction. In the other direction, however, one would get additional reflection losses, which are circumvented by using a ring cavity. The non-collinear angle required for broadband phase matching ($\alpha = 4.5°$) is set by adapting the vertical displacement of the pump beam from the center of the large lens L_1 ($d = 75$ mm, $f = 200$ mm) using a periscope. The visible light is then generated by using type-I difference-frequency generation (DFG) in a BBO crystal ($\theta = 39°$, $L = 2$ mm, Brewster-cut), which is placed in the first focus of our cavity. To satisfy the phase matching condition, the Poynting vector walk-off compensation (PVWC) geometry is chosen. In this configuration, the Poynting vectors of pump and signal point in approximately the same direction, resulting in a longer spatial overlap and improved beam profiles for the generated visible light. However, it has the disadvantage that a parasitic generation of the second harmonic is phase matched simultaneously in the BBO crystal at a certain signal wavelength, here at about 600 nm. This becomes visible later in the measured data as a dip in the output power. A well-defined intracavity dispersion is realized by a BK7 substrate, the nonlinear crystals, and dedicated double-chirped mirror pairs (DCMs), which were already used in [11]. Thus, some parametric fluorescence generated in the DFG process is temporally broadened by a certain amount during propagation in the cavity. After one round-trip, only those wavelengths are amplified which arrive in the BBO crystal at the same time as the short ultraviolet pump pulse. Hence, tuning the visible wavelength becomes possible by changing the resonator length within a range of approximately 200 µm, as this alters the round-trip time of the different colors, resulting in the amplification of a new spectral region of the dispersed parametric fluorescence, while the gain mechanism ceases at the previous wavelength. A detailed description of the complex NOPO dynamics can be found in [17]. Measurements of the resulting tuning behavior are performed both with and without an output coupling mirror for the visible pulses by exchanging mirror M_8 from an high reflector to a mirror with 5% transmission.

An extension of the spectral tuning range towards shorter wavelengths is possible via sum-frequency generation (SFG) between the NOPO pulses and residual light from the MOFA system with an average power of approximately 3.2 W. A suitable nonlinear crystal is KDP ($\theta = 75°$, $L = 2$ mm, Brewster-cut), which supports the generation of broadband tunable radiation in the

Optics EXPRESS

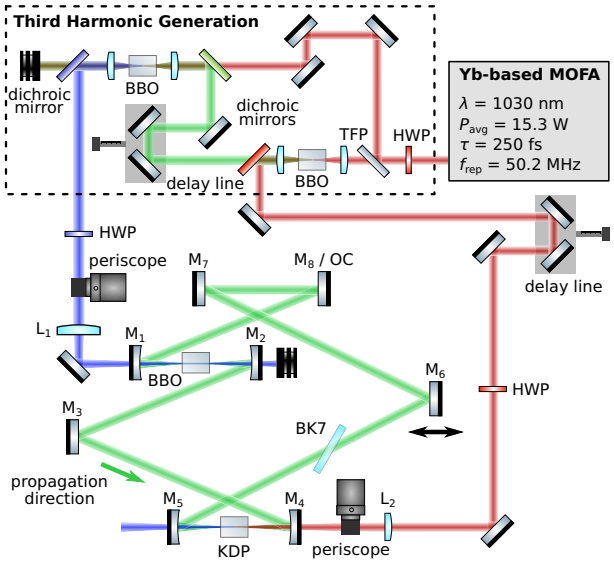

Fig. 1. Schematic sketch of the experimental setup. HWP: half-wave plate, TFP: thin-film polarizer. The pump laser as well as the third harmonic generation setup are shown in the upper part of the sketch. The lower part displays the ring cavity, which consists of curved (ROC = −150 mm) and plane inhouse designed DCMs ($M_1 - M_8$) with a high reflectivity from 400 to 700 nm, a BK7 substrate placed at Brewster's angle (L = 6.5 mm), and two nonlinear crystals, BBO (θ = 39°, L = 2 mm) and KDP (θ = 75°, L = 2 mm), both cut at Brewster's angle. The resonator length can be varied by moving M_6. Furthermore, M_8 can be replaced by an output coupling mirror (OC). The ultraviolet and near-infrared beams are focused into the resonator using a periscope and the lenses L_1 (f = 200 mm) and L_2 (f = 300 mm), respectively. Both non-collinear angles lie in the vertical plane and are therefore not visible in the sketch.

near-UV region by using a type-II process with a large non-collinear angle of about 11°. This way, the phase matching condition can be satisfied from approximately 505-700 nm for the visible driving pulses, which enables the generation of near-UV light in a range of 339-417 nm. The corresponding phase matching curve is shown in Fig. 2, where an effective crystal length of 580 µm is assumed, which corresponds to the calculated spatial interaction length inside the KDP crystal. Due to difficulties in the manufacturing process of thin crystals cut at Brewster's angle, a longer crystal with a thickness of 2 mm is used in this work. However, this is not expected to have any significant impact on the performance of the system, as the beams separate quickly due to the large angles after the interaction area. To maximize the conversion efficiency, which strongly depends on the intensity of the input pulses, the crystal is placed in the second focus of the ring cavity. Due to the large non-collinear phase-matching angle in the KDP, the pulses leave the cavity below mirror M_5, and no additional output coupler is needed. Again, the non-collinear angle is set using a periscope, while the temporal overlap is aligned with a delay line (see Fig. 1). As mentioned above, tuning of the NOPO wavelength is achieved by varying the cavity length in a range of 200 µm, which corresponds to a group delay (GD) of about 670 fs. Thus, the time delay of the 1030 nm pulses used in the SFG would need to be adjusted during the tuning process to maintain the temporal overlap with the NOPO pulses. However, this would reduce the maximum achievable tuning speed. Therefore, the group delay dispersion (GDD) in the short arm of the resonator between M_2 and M_4 is minimized and the cavity length is varied by moving a mirror in the long arm (e.g. M_6), which results in approximately equal arrival times of the NOPO pulses

Optics EXPRESS

in the KDP crystal. This approach allows to use a constant temporal delay of the 1030 nm pulses over the whole spectral range. A change of the near-UV wavelength is then only limited by the maximum achievable tuning speed of the NOPO pulses.

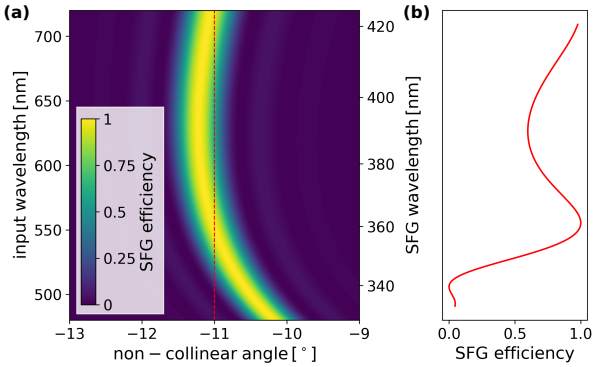

Fig. 2. Phase matching in KDP. (a) Normalized conversion efficiency of sum-frequency mixing between o-polarized visible and e-polarized 1030 nm pulses in KDP (θ = 75°, L = 580 µm) as a function of the NOPO wavelength and the non-collinear angle. (b) Intersection along the dashed red line in the left plot.

3. Results

Figure 3 shows the spectrum and average output power of the generated near-UV radiation for different cavity lengths. Femtosecond pulses with a center wavelength from approximately 333-413 nm are generated by varying the cavity length in a range of about 200 µm. The maximum average output power of 90 mW is reached at a wavelength of 369 nm. In principle, even higher powers are achieved in the nonlinear mixing process, however, the s-polarized UV light experiences high losses when leaving the KDP crystal cut at Brewster's angle, resulting in the usable output power shown in Fig. 3(b). The significant drop in power at a wavelength of about 378 nm can be attributed to a simultaneous collapse in the visible intracavity power caused by the parasitic second harmonic generation in the PVWC configuration. Furthermore, the spectral tuning curve exhibits slight jumps, especially pronounced beyond 400 nm. These can be attributed to the dispersion ripples of the used DCMs, causing the wavelength resolved round-trip GDD to approach zero within this range. More detailed information on the tuning characteristics of NOPOs can be found in [9,17]. The long-term stability of the near-UV radiation close to maximum output power is investigated over a period of about 35 min, resulting in a rms noise of approximately 1.1 %. In addition, a slow degradation in output power of 0.3 mW per minute is observed. This decrease can be attributed to a simultaneous reduction in ultraviolet pump power, primarily caused by thermal misalignment of specific mirror mounts within the third harmonic generation setup. It can therefore be easily removed by implementing appropriate cooling or motorization of those mirror mounts. Another important parameter for later applications is the beam pointing of the created near-UV pulses. Since these are generated in a non-collinear process, spatial walk-off is expected for different wavelengths when leaving the resonator. For the phase-matching geometry used in this work, an angular variation of approximately 16 mrad is measured when tuning the wavelength from 349 nm to 409 nm, which would result in a spatial displacement of 1.6 mm when collimating the beam with a lens with a focal length of 100 mm. It must therefore be taken into account in follow-up experiments.

The duration of the UV pulses is determined by using a cross-correlation technique. In this process, DFG between the near-UV radiation and an auxiliary beam at different delays is used to

Optics EXPRESS

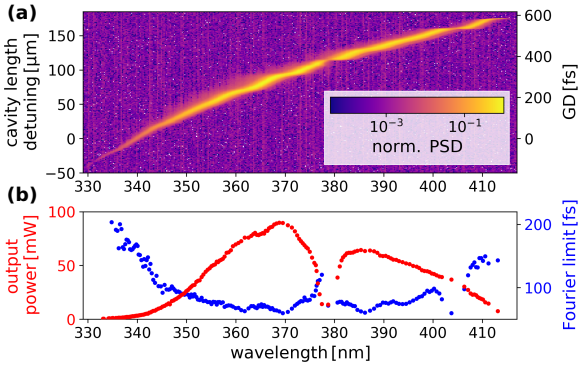

Fig. 3. Tuning behavior in the near UV. (a) Normalized power spectral density (PSD) as a function of wavelength and relative cavity length detuning. (b) Average output power and Fourier limit of the near-UV pulses as a function of wavelength. The dip in power at 378 nm is due to the PVWC configuration chosen to operate the NOPO.

receive a down-converted signal that can be measured with a photodiode. If the pulse duration of the auxiliary beam is known, the duration of the near-UV pulses can be extracted from the measured signal [18,19]. The setup used for the cross-correlation is shown in Fig. 4(a). As an auxiliary beam, the residual near-infrared light from the non-collinear SFG is chosen. The visible cross-correlation signal is then generated in a Brewster-cut BBO crystal ($\theta = 26.94°$, $L = 0.5$ mm). Fig. 4(b) shows such a measurement for a pulse at 371 nm, where the duration of the cross-correlation signal is determined to be 434 fs. Assuming sech^2 shapes for the two inputs, a pulse duration of 231 fs in the near-UV is deduced from the measured data at a Fourier limit of 67 fs (see Fig. 3(b)). Thus, further shortening of the pulse duration is possible by subsequent chirp compensation. Additional measurements are performed at various wavelengths distributed over the tuning range, resulting in pulse durations from 158-240 fs assuming sech^2 input pulses.

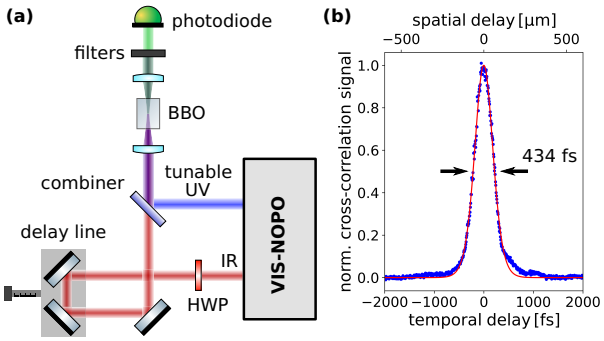

Fig. 4. (a) Setup for determining the near-UV pulse duration. The cross-correlation signal is generated via difference-frequency mixing in a BBO crystal ($\theta = 26.94°$, $L = 0.5$ mm, Brewster-cut). Before measuring the visible light with a photodiode, filters (KG1 and OG530) are used to block remaining input radiation. (b) Measured cross-correlation signal (blue dots) as a function of delay between near-infrared (1030 nm) and ultraviolet pulses (371 nm). In addition, the theoretically expected cross-correlation signal calculated under the assumption of sech^2 input pulses is shown as a red curve.

Instead of a single output in the near UV, two synchronized tunable beams can be realized by replacing the plane cavity mirror M_8 by a 5 % output coupler for the NOPO pulses. The

Optics EXPRESS

corresponding measurement is shown in Fig. 5. This way, visible light from 449-690 nm is generated simultaneously with the tunable UV pulses from 340-413 nm, with output powers up to 232 mW and 59 mW, respectively. The reduced ultraviolet power can be attributed to the higher losses for the visible pulses. Various ratios of output power in the two spectral regions can be realized by selecting different output couplers. Furthermore, Fig. 5 shows the recorded beam profile of the near-UV radiation at maximum output power. Despite a slight ellipticity, which was already observed in [11] for the visible NOPO output, the pulses exhibit a good Gaussian shape.

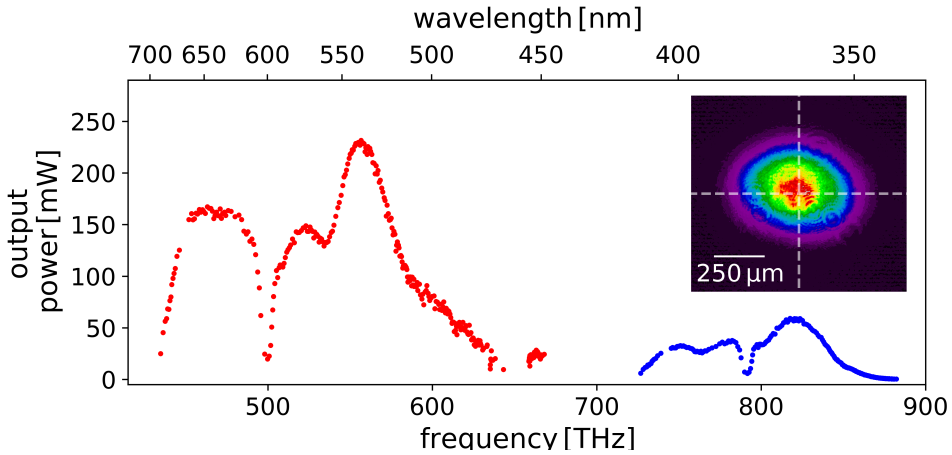

Fig. 5. Average output power of both the visible NOPO operated with a 5 % output coupler (red data) and the near-UV pulses generated through intracavity SFG (blue data) as a function of frequency. The upper axis shows the corresponding wavelength values. Inset: Beam profile of the focused (f = 500 mm) near-UV radiation at maximum output power.

Due to the non-collinear phase matching geometry, the wavelength of visible and ultraviolet pulses can be varied by changing the resonator length only. This allows for rapid wavelength changes. Fig. 6 shows a stroboscopic measurement of the near-UV tuning curve. In order to realize the rapid periodic resonator length change, one of the plane cavity mirrors is mounted on a piezoelectric actuator (PK2FVF1 from Thorlabs), which is driven by a sinusoidal voltage and

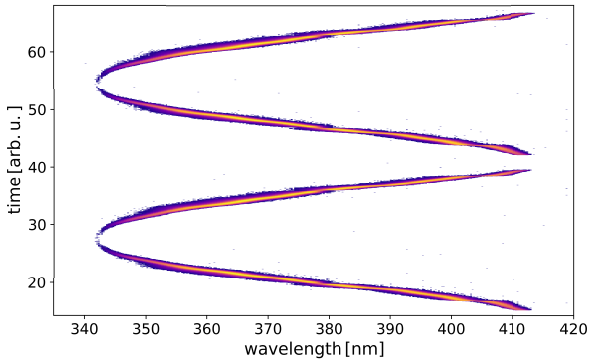

Fig. 6. Stroboscopic measurement of the fast tunability of near-UV pulses. The center wavelength is varied by changing the cavity length with a piezoelectric actuator at 43.9 Hz, which is close to one-third of the sampling frequency of the used spectrometer (131.6 Hz). Hence, only every third sample from the spectrometer data is shown.

Optics EXPRESS

allows for wavelength variations over the whole spectral range with 43.9 Hz. For the measurement, the signal is sampled at 131.6 Hz, which corresponds to the acquisition frequency of the used spectrometer (HR4000CG-UV-NIR from Ocean Optics). Furthermore, the integration time is set to the lowest possible value of 10 µs in order to minimize smearing of the recorded spectra due to the rapid wavelength changes. Sampling is thus done at a frequency that is close, but not exactly, to three times the cavity length modulation. Because of this, three sampling points per modulation cycle are obtained, which is why only every third sample from the spectrometer data is used for the measurement shown in Fig. 6. Higher tuning speeds are not achieved due to limitations in the driving electronics of the used piezoelectric actuator. However, it must be emphasized that there is no physical limitation for the tuning speed besides the mass of the mirror and its driver.

4. Conclusion and outlook

In this work, we have demonstrated for the first time, to the best of our knowledge, the simultaneous generation of broadband, rapidly tunable femtosecond pulses in the visible and near-ultraviolet spectral range using a non-collinear optical parametric oscillator. The system allows the use of a single output as well as the generation of two synchronized pulse trains. In the former case, ultraviolet light is generated over a broad range, from 333-413 nm, with high average output power, up to 90 mW. In the latter case, both values are slightly reduced due to the higher output coupling losses, which results in near-UV pulses from 340-413 nm with average output powers up to 59 mW. The additional visible output provides radiation from 449-690 nm with powers up to 232 mW. Measurements of the near-UV pulse duration are performed at various wavelengths distributed over the tuning range using cross-correlation, resulting in values between 158-240 fs. Furthermore, the fast tunability of both spectral ranges is demonstrated with a frequency of 43.9 Hz, where the tuning speed is limited by the used electronics only.

Due to the use of parametric processes for generating tunable laser pulses, the system has good power scalability. In addition to enhancing output power, further improvements can be made to the conversion efficiency. For instance, the beam quality of the 1030 nm pulses utilized in the non-collinear SFG has suffered due to the preceding generation of the second harmonic. Thus, implementing proper beam cleaning techniques would likely result in an increase of conversion efficiency. Alternatively, the availability of higher fundamental power would also allow the use of infrared pulses delivered directly from the MOFA system. Moreover, it would be possible to replace the KDP crystal cut at Brewster's angle with a broadband anti-reflection coated crystal. This substitution would lead to reduced losses for the infrared input beam and the generated near-UV pulses, as both suffer from significant reflection losses in the current setup due to their s-polarization. To obtain a more uniform power distribution across the covered spectral range, the tangential phase matching geometry (TPG) could be utilized for generating the NOPO pulses [12,17]. In this configuration, no parasitic second harmonic generation occurs compared to PVWC. However, when using TPG, the signal pulses typically show poor beam quality. This drawback can be mitigated by selecting a weak focus for the DFG. To counteract the resultant decrease in intensity, higher pump powers must be used, which would require an update to our MOFA system.

Together with previous work done in the author's group [9,11,12], it is now possible to cover the entire region from 333-1191 nm without any gaps with fast tunable sources. This provides a solid basis for the application of new methods in the field of real-time spectroscopy or imaging.

Funding. Deutsche Forschungsgemeinschaft (EXC 2122 Project ID 390833453, MO 850/ 31-1); Horizon 2020 Framework Programme (Marie Sklodowska-Curie Agreement No. 713694).

Disclosures. The authors declare no conflicts of interest.

Data availability. Data underlying the results presented in this paper are not publicly available at this time but may be obtained from the authors upon reasonable request.

Optics EXPRESS

References

1. J. A. Giordmaine and R. C. Miller, "Tunable Coherent Parametric Oscillation in $LiNbO_3$ at Optical Frequencies," Phys. Rev. Lett. **14**(24), 973–976 (1965).
2. S. Harris, "Tunable optical parametric oscillators," Proc. IEEE **57**(12), 2096–2113 (1969).
3. M. Ghotbi, A. Esteban-Martin, and M. Ebrahim-Zadeh, "Tunable, high-repetition-rate, femtosecond pulse generation in the ultraviolet," Opt. Lett. **33**(4), 345–347 (2008).
4. C. Gu, M. Hu, J. Fan, Y. Song, B. Liu, L. Chai, C. Wang, and D. T. Reid, "High power tunable femtosecond ultraviolet laser source based on an Yb-fiber-laser pumped optical parametric oscillator," Opt. Express **23**(5), 6181–6186 (2015).
5. M. Ghotbi, A. Esteban-Martin, and M. Ebrahim-Zadeh, "BiB_3O_6 femtosecond optical parametric oscillator," Opt. Lett. **31**(21), 3128–3130 (2006).
6. K. C. Burr, C. L. Tang, M. A. Arbore, and M. M. Fejer, "High-repetition-rate femtosecond optical parametric oscillator based on periodically poled lithium niobate," Appl. Phys. Lett. **70**(25), 3341–3343 (1997).
7. C. F. O'Donnell, S. C. Kumar, P. G. Schunemann, and M. Ebrahim-Zadeh, "Femtosecond optical parametric oscillator continuously tunable across 3.6-8 μm based on orientation-patterned gallium phosphide," Opt. Lett. **44**(18), 4570–4573 (2019).
8. J. Fan, C. Gu, C. Wang, and M. Hu, "Extended femtosecond laser wavelength range to 330 nm in a high power LBO based optical parametric oscillator," Opt. Express **24**(12), 13250–13257 (2016).
9. T. Lang, T. Binhammer, S. Rausch, G. Palmer, M. Emons, M. Schultze, A. Harth, and U. Morgner, "High power ultra-widely tuneable femtosecond pulses from a non-collinear optical parametric oscillator (NOPO)," Opt. Express **20**(2), 912–917 (2012).
10. G. M. Gale, M. Cavallari, and F. Hache, "Femtosecond visible optical parametric oscillator," J. Opt. Soc. Am. B **15**(2), 702–714 (1998).
11. R. Mevert, Y. Binhammer, C. M. Dietrich, L. Beichert, J. R. C. d. Andrade, T. Binhammer, J. Fan, and U. Morgner, "Widely tunable, high-power, femtosecond noncollinear optical parametric oscillator in the visible spectral range," Photonics Res. **9**(9), 1715–1718 (2021).
12. Y. Binhammer, T. Binhammer, R. Mevert, T. Lang, A. Rück, and U. Morgner, "Fast-tunable femtosecond visible radiation via sum-frequency generation from a high power NIR NOPO," Opt. Express **29**(14), 22366–22375 (2021).
13. T. Lang, T. Binhammer, S. Rausch, G. Palmer, M. Emons, M. Schultze, A. Harth, and U. Morgner, "Rapidly Spectral Ramping of an ultra-wide Tuneable Femtosecond Non-collinear Optical Parametric Oscillator (NOPO) with high average output power," in *Lasers, Sources, and Related Photonic Devices (2012)*, paper AT2A.2, (Optica Publishing Group, 2012).
14. A. Pape, T. Binhammer, Y. Khanukaeva, T. Lang, J. Ahrens, O. Prochnow, and U. Morgner, "Ultrafast spectral switching of a Non-collinear Optical Parametric Oscillator (NOPO)," in *International Conference on Ultrafast Phenomena (2016)*, paper UW4A.43, (Optical Society of America, 2016).
15. L. Beichert, Y. Binhammer, J. R. C. Andrade, R. Mevert, A.-K. Kniggendorf, B. Roth, and U. Morgner, "Real-time stimulated Raman spectroscopy with a non-collinear optical parametric oscillator," Opt. Express **29**(20), 31499–31507 (2021).
16. M. Höhl, B. Roth, U. Morgner, and M. Meinhardt-Wollweber, "Efficient procedure for the measurement of preresonant excitation profiles in UV Raman spectroscopy," Rev. Sci. Instrum. **88**(7), 073105 (2017).
17. T. Lang, "Ultrashort laser pulses from optical parametric amplifiers and oscillators," Ph.D. thesis, Gottfried Wilhelm Leibniz Universität Hannover (2014).
18. A. Weiner, "Effect of group velocity mismatch on the measurement of ultrashort optical pulses via second harmonic generation," IEEE J. Quantum Electron. **19**(8), 1276–1283 (1983).
19. A. Baronavski, H. Ladouceur, and J. Shaw, "Analysis of cross correlation, phase velocity mismatch and group velocity mismatches in sum-frequency generation," IEEE J. Quantum Electron. **29**(2), 580–589 (1993).

89.245.22.220 {ts '2023-11-20 01:43:46'}